ELSEVIER

Polymer 42 (2001) 9771–9782

polymer

www.elsevier.com/locate/polymer

Transient interfacial instability in bilayer polymer films as observed by neutron reflectivity studies

M. Hayashi[a], T. Hashimoto[a,*], M. Weber[b], H. Grüll[c,1], A.R. Esker[c,2], C.C. Han[c], S.K. Satija[d]

[a]*Department of Polymer Chemistry, Graduate School of Engineering, Kyoto University, Yoshida-honmachi, Sakyo-ku, Kyoto 606-8501, Japan*
[b]*BASF Aktiengesellschaft, Polymer Research Laboratory, Engineering Plastics, D-67056 Ludwigshafen, Germany*
[c]*Polymers Division, National Institute of Standards and Technology (NIST), Gaithersburg, MD 20899, USA*
[d]*NIST Center for Neutron Research, National Institute of Standards and Technology (NIST), Gaithersburg, MD 20899, USA*

Received 22 March 2001; received in revised form 28 June 2001; accepted 13 July 2001

Abstract

Fundamental processes associated with reactive blending were explored for a system composed of polyamide (PA) and deuterated polysulfone having a reactive phthalic anhydride end group (R) (dPSU-R) diluted with a low molecular weight hydrogenous polysulfone (low-hPSU) by neutron reflectivity (NR). By preparing bilayer films composed of a mixed film of dPSU-R/low-hPSU and a PA film, an intriguing phenomenon was observed in NR studies during the thermal annealing of the sample. This phenomenon can be described as a transient instability of the interface between the PA layer and the dPSU-R/low-hPSU layer during annealing at temperatures high enough to allow chemical reactions to occur between the dPSU-R end groups and the terminal amino groups of PA. The signature for the interfacial instability was a transient disappearance of the NR fringes followed by a subsequent recovery of the fringes during additional annealing at high temperatures. The driving force for this phenomenon is rapid interdiffusion of a small, low molecular weight fraction of low-hPSU into the PA layer. A consequence of the rapid interdiffusion is an attendant Kirkendall shift of the interfacial position as the PSU layer shrinks. The magnitude of this special Kirdendall effect accompanying the interfacial instability is directly controlled by the amount of the miscible low molecular weight fraction of low-hPSU present in the normally immiscible PSU/PA pair. © 2001 Published by Elsevier Science Ltd.

Keywords: Neutron and X-ray reflectivity; Reactive blending; Polymer interface

1. Introduction

Reactive blending of an immiscible polymer pair of polymers A and B involves, in principle, blending A and B along with the corresponding reactive polymers (A^* and B^*). Either graft or block copolymers of A^* and B^* formed during blending then act as a compatibilizer for the blend through their localization at the interface between phase separating domains rich in A and A^* and those rich in B and B^*. Fundamental steps of this reactive blending process are the diffusion of A^* and B^* to the interface, the reaction of A^* and B^*, and the subsequent localization of the copolymers formed at the interface [1–10]. This report contains a neutron reflectivity (NR) study of bilayer thin films composed of a uniform mixture of A and A^* (A/A^*) and B and B^* (B/B^*). The bilayer films, hereafter designated Air//A/A^*//B/B^*//Si, contain three macroscopic interfaces, i.e. these interfaces are between air and A/A^*, A/A^* and B/B^*, and B/B^* and the silicon wafer. The notation for these interfaces includes the use of '//' to designate a macroscopic interface and '/' to indicate a uniform mixture of two components.

Previous reports exist for the NR analysis of a reactive blending process [9]. In that study, deuterium labeled polysulfone with a reactive phthalic anhydride end group (dPSU-R) could be diluted by non-reactive normal polysulfone (hPSU) and was allowed to react with an amino terminated polyamide (PA) in the bilayer specimen Si//dPSU-R/hPSU//PA//Air. Using the notation developed above, the system explored in Ref. [9] corresponds to Si//A/A^*//B^*//Air. Similar to that study, we also considered the control experiments, Si//A^*//B^*//Air and Si//A//B//Air. An important detail of that work was the use of dPSU (dPSU-R without a reactive end group), dPSU-R, and hPSU possessing comparable molecular weights which were known to be miscible at the molecular level [11]. Under these conditions,

* Corresponding author. Tel.: +81-75-753-5604; fax: +81-75-753-4864.
E-mail address: hashimoto@alloy.polym.kyoto-u.ac.jp (T. Hashimoto).
[1] Present address: Philips Research Laboratories, 5656 AA Eindhoven, The Netherlands.
[2] Present address: Virginia Tech, Department of Chemistry, Blacksburg, VA 24061-0212, USA.

0032-3861/01/$ - see front matter © 2001 Published by Elsevier Science Ltd.
PII: S0032-3861(01)00519-5

Table 1
Characteristics of polymers used in this study

Polymer	N_w [a]	N_w/N_n [a]	End group (%)			
			PhAh	OH	Cl	OCH_3
hPSU[b]	86	2.52	–	–	50	50
Low-hPSU[c]	5	1.70	–	0.5	99.5	–
dPSU[d]	58	3.51	–	3	97	–
Low-dPSU[e]	5	1.58	–	1.4	98.6	–
dPSU-R[f]	80	6.27	50	35	15	–
PA[g]	3.3×10^4 [h]	3.90[h]	–	–	–	–

[a] Measured with size exclusion chromatography.
[b] Protonated polysulfone with a relatively large molecular weight.
[c] Low molecular weight protonated polysulfone.
[d] Deuterated polysulfone with a relatively large molecular weight.
[e] Low molecular weight deuterated polysulfone.
[f] Deuterated polysulfone with reactive (phthalic anhydride) end group.
[g] Polyamide, Grilamide®, EMS, Switzerland.
[h] Since an average degree of polymerization is not well defined, we indicated here weight average molecular weight M_w and M_w/M_n.

the results indicate an increase in the interfacial width $W_{I,obs}$ with time upon the thermally induced reaction of the bilayer film specimens at high annealing temperatures with a consequential formation and localization of a block copolymer monolayer, dPSU-*b*-PA, at the interface between the PSU and PA layers [9].

As an extension of our previous work, hPSU is replaced by a substantially lower molecular weight hydrogenous polysulfone (low-hPSU). The motivation for studies of Si//dPSU-R/low-hPSU//PA//Air is twofold. The replacement of hPSU by low-hPSU should induce the following two effects: (a) an increased mobility of dPSU-R in the PSU matrix, and (b) an anticipated enhancement of partial miscibility between PSU and PA resulting from the decrease in the average molecular weight of the PSU phase upon the substitution of low-hPSU for hPSU. Both the scientific and technological implications these factors could have on reactive blending processes provided the impetus for this study.

During the course of this new study, an unexpected anomaly appeared in the time dependent evolution of the NR curves during the reactive blending process. This anomaly consisted of a decrease in the amplitude and number of observed reflectivity fringes at early annealing times, followed by the recovery of both the amplitude and number of fringes at later times. This observation reflects a transient instability of the interface between the PSU and PA phases and a subsequent relaxation of the instability with a time scale on the order of 300 min for the system. To the best of our knowledge, this is the first time such an extreme demonstration of this phenomenon has been reported. Elements of the transient instability were observed in a previous study (Si//dPSU-R//PA//Air) at short annealing times (10 min, 210°C), while other cases did not show any hint of this phenomenon (Si//dPSU-R/hPSU//PA//Air and Si//dPSU//PA//Air) [9]. In order to explore the origin of this phenomenon, additional NR experiments corresponding to the non-reactive system, e.g. Si//dPSU/low-hPSU//PA//Air, as well as those for single layers of Si//dPSU-R/low-hPSU//Air and Si//dPSU/low-hPSU//Air, were performed. A primary objective of this paper is to describe details of a new intriguing finding regarding the transient instability of the interface and to explore its possible physical origins.

2. Experimental

2.1. Polymers used in this work

All the PSU and PA materials used for this study were synthesized and characterized by BASF Aktiengesellschaft, Germany [12–14]. Characterization data for these samples are summarized in Table 1. The chemical structures of polysulfone (hPSU, dPSU, dPSU-R, low-dPSU and low-hPSU), and phthalic anhydride end groups (–R) and Grilamide (PA) as well as the block copolymer dPSU-*b*-PA, formed by the interfacial reaction, are shown in Fig. 1. Note that the chemical structure of low-hPSU is identical to that of hPSU in Ref. [10], except for the structure of the end group (Table 1).

For comparison, experiments were carried out using well-understood systems to reproduce elements of the significant features observed for the PSU//PA system. These studies utilized two different molecular weights[3] of deuterium labeled polystyrene samples dPS (weight average molecular weight, $M_w = 40 \times 10^3$, polydispersity, $M_w/M_n = 1.02$, Polymer Laboratories, Inc. and $M_w = 1.55 \times 10^3$, prepared by Prof. Jimmy Mays, Univeristy of Alabama) and two different molecular weight of hydrogenous hPS ($M_w = 39 \times 10^3$, $M_w/M_n = 1.02$, Polymer Laboratories, Inc. and $M_w = 1.11 \times 10^6$, $M_w/M_n = 1.15$, Polymer Source, Inc.).[4] In addition, these samples utilized isopentylcellulose cinnamate (IPCC) identical to that used elsewhere [15].

2.2. Preparation of samples for neutron reflectivity, X-ray reflectivity, and small angle neutron scattering

The systems studied and the experimental methods applied to each system are summarized in Table 2, where the experimental conditions such as annealing temperature, and time are also shown and the notations SANS and XR correspond to small-angle neutron scattering and X-ray reflectivity, respectively. Uniform polysulfone films of a

[3] According to ISO 31-8, the term 'molecular weight' (M_w) has been replaced with 'relative molecular mass' symbol $M_{r,w}$. The conventional notation, rather than ISO notation, has been employed for this article.

[4] Certain commercial materials and instruments are identified in this article to adequately specify the experimental procedure. In no case does such identification imply recommendation or endorsement by the National Institute of Standards and Technology; nor does it imply that materials or equipment identified are necessarily the best available for the purposes.

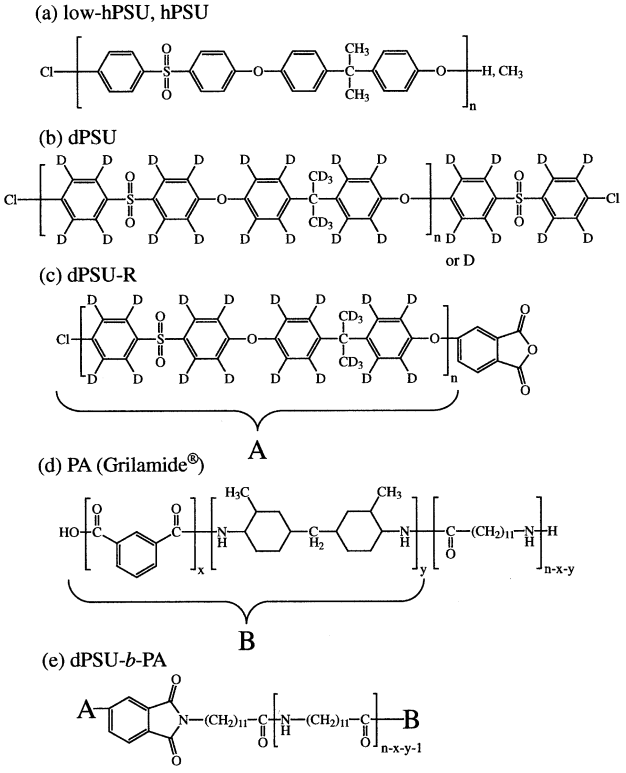

Fig. 1. Chemical structures for the polymers studied in this work.

thickness $d \approx 600$ Å listed in Table 2 (dPSU-R/low-hPSU, dPSU/low-hPSU, low-hPSU, dPSU-R and dPSU) were prepared for NR and XR by spincoating from chlorobenzene solutions onto silicon wafers (5 mm thick, 75 mm diameter) obtained from Semiconductor Processing, Inc.,[4] Boston, MA, USA. Prior to spincoating, the silicon substrates were cleaned by an ozone plasma for 20 min, and were then boiled for 1.5 h at 90°C in a bath of concentrated H_2SO_4/H_2O_2 (70/30 vol%/vol%). The oxide layer on the substrates was then stripped off in an aqueous HF solution with a mass fraction of 3% HF for 3 min. In order to stabilize the hydrophobic surface, the wafers were immersed in an aqueous solution of 40% NH_4F with concentration of 40 mass fraction % NH_4F. To complete the bilayer specimens, a thick film of PA ($\approx 20 \times 10^3$ Å) was spincoated onto another hydrophilic Si wafer out of a 1,1,1,3,3,3-hexafluoro-2-propanol (HFIP) solution with 1 wt% PA concentration. Upon immersing this wafer into water, the PA floats off the wafer onto the water surface and is subsequently picked up with the target wafer, on which the PSU sample had been spincoated. The prepared bilayers were then dried for one day under vacuum at 50°C. Bilayer specimens prepared in this manner are referred to as the initial state prior to annealing (designated as '0 min' in the figures shown later). Specimens for SANS experiments were prepared as follows: The mixtures were dissolved in appropriate solvents, i.e. chlorobenzene for dPSU-R/low-hPSU and HFIP for low-hPSU/PA, to get homogeneous 5 wt% solutions. These solutions were initially precipitated into hexane and later into ethanol multiple times. Afterwards, the precipitate was filtered using paper filters and dried at 80°C for one day under vacuum. Subsequently, the precipitated mixture was melt-pressed and molded at 160°C under ca. 4 MPa for 5 min into disks with a thickness of 0.5 mm and a diameter of 15 mm.

For comparison, two other samples were also prepared. The first was an Air//hPS ($M_w = 39 \times 10^3$)//dPS ($M_w = 40 \times 10^3$)//Si sample, where the dPS layer was spincoated onto a hydrophobic HF etched silicon wafer from toluene, while the hPS layer was floated on top to complete the bilayer. The second sample was comprised of Air//IPCC (800 Å)//dPS ($M_w = 1.55 \times 10^3$)/hPS ($M_w = 1.11 \times 10^6$)//Si, where the dPS/hPS was spincoated and an 80 layer Langmuir–Blodgett (LB) film of IPCC was deposited on top (Nima Technologies, Ltd). The LB film was subsequently photo cross-linked by exposure to UV irradiation (wavelengths > 280 *nm*) to form a network.

2.3. NR, XR, and SANS measurements

XR measurements were performed at the NIST Center for Neutron Research (NCNR), NIST, Gaithersburg, MD, USA. XR as well as NR were applied to the spincoated single layer polymer films to determine the thicknesses and roughnesses of the layers by irradiating X-ray or neutron beam from the air side. The specularly reflected X-rays (or neutrons) were detected using a scintillation counter, as a function of the magnitude of the scattering vector **q**, which is defined as

$$q = |\mathbf{q}| = (4\pi/\lambda)\sin\theta, \tag{1}$$

where θ is the angle of incidence and reflection relative to the sample surface for the beam with wavelength, $\lambda = 1.54$ Å.

NR measurements were performed on the NG7 reflectometer at the NCNR. The bilayer samples mentioned in Section 2.2 were annealed at temperatures above the glass transition temperature and subsequently quenched back to room temperature for the experiments. For the NR measurements, the samples were inverted, i.e. the unpolished bottom Si surface was facing up and the polished Si surface in contact with the bilayer faced down toward the horizontal sample stage of the NG7 reflectometer. In this configuration, it was possible to measure the reflectivity of the sample from the Si//polymer interface through the polished edge of the wafer and avoid absorbance of the incident neutron beam by the thick PA layers. Thus, the incident neutron beams irradiated the sample from the Si side and the reflected neutrons were detected with a pencil neutron detector as a function of q (Eq. (1)). In general, the reflectivity itself is obtained by dividing the measured reflected intensity by that in the range of q where total reflection is observed. As absorbance problems are not so critical for finite thickness samples, the two comparative samples based on PS were measured from the air/side.

SANS experiments were performed on the NG1 SANS

Table 2
Samples and experimental conditions

Sample	Experiments	Experimental conditions
dPSU-R/low-hPSU (mass ratio 30/70)	SANS (mixture) NR, XR (single layer)	(118–190°C), single phase 190°C, (0–30 min)
dPSU/low-hPSU (mass ratio 30/70) low-dPSU	NR, XR (single layer) XR (single layer)	190°C (0–10 min) 160°C (120 min)
dPSU-R/low-hPSU (mass ratio 30/70)//PA	NR (bilayer)	(150–190°C), (0–320 min)
dPSU/low-hPSU (mass ratio 30/70)//PA	NR	160, 190°C (0–90, 0–50 min)

diffractometer at the NCNR in order to determine the miscibility of dPSU-R/low-hPSU mixtures (or dPSU/low-hPSU). The prepared specimens were sandwiched between two copper windows with a thickness of 0.5 mm, and set in the copper cell designed for the sample holder of the instrument. The in situ measurements of the scattering intensity distribution from the samples were performed as a function of annealing temperature. The experimental procedure and data analyses detailed elsewhere were followed [16]. The data were corrected for empty cell scattering and incoherent scattering, and then, the scattering intensities were converted to absolute values.

2.4. DSC measurements

Differential scanning calorimetry (DSC) measurements were performed using a Du Pont 2000 instrument at a heating rate of 20 K/min. The glass transition temperatures T_gs were obtained from the second run. The T_g value is always taken to be the temperature where half the increase in the heat capacity has occurred. The results are summarized in Table 3. All experiments in this study concerning the effects of annealing on NR and XR profiles were conducted above the T_gs of the respective components and/or systems.

3. Results

3.1. Characterization of the miscibility of dPSU-R and low-hPSU

The SANS profiles for the binary mixture of dPSU-R and low-hPSU with a composition of 30 wt%/70 wt%, respectively, showed the mixture is uniphasic. The profiles in the one-phase region were investigated as a function of temperature and the experimental profiles were fit with theoretical profiles using the random phase approximation (RPA) [17] to determine the Flory–Huggins interaction parameter [18], $\chi(T)$, as a function of temperature (T),

$$\chi(T) = -0.618 + 114.8/T. \quad (2)$$

This result is consistent with an upper critical solution temperature (UCST) phase diagram. From the temperature dependence of χ, the mean-field spinodal temperature is calculated as $T_s = -86.2$°C, which indicates that this mixture is totally miscible over the entire temperature range studied here. In addition, the binary mixture of dPSU and low-hPSU with a composition of 30 wt%/70 wt%, respectively, is also completely miscible under the experimental conditions studied. These results are consistent with the spincoated single layer films of dPSU-R/low-hPSU (30 wt%/70 wt%) and dPSU/low-hPSU (30 wt%/70 wt%) existing in a one-phase state.

Table 3
DSC measurements of glass transition temperatures (T_g)

Specimens	T_g (°C)
hPSU	188
low-hPSU	94
dPSU	180
dPSU-R	174
PA	113
dPSU-R/low-hPSU	116
dPSU/low-hPSU	133

3.2. NR and XR characterization of single layers of dPSU-R/low-hPSU and dPSU/low-hPSU on silicon

The NR and XR data were fit using a standard multilayer fitting routine for the scattering length densities (SLD) [19]. Fig. 2 shows NR (part a) and XR (part b) data (open circles), and best-fit curves (solid lines) for several different annealing times at 190°C.[5] The corresponding SLD profiles for the single layer of dPSU-R/low-hPSU (30 wt%/70 wt%) on a Si substrate (Si//dPSU-R/low-hPSU//Air) are provided as insets. The NR and XR profiles are largely time independent at least over the time scale of our observations at 190°C, which is normal as we expect. Nearly identical NR and XR results were obtained for the dPSU/low-hPSU (30 wt%/70 wt%) single layer (Si//dPSU/low-hPSU//Air) at 190°C, so this data is omitted. The SLD profile for NR has a dip near the Si interface, which indicates that the protonated component, i.e. low-hPSU, adsorbs. In contrast, the electron density profile (analogous to SLD for neutrons) for XR does not show this trend because there is not a significant electron density difference between dPSU-R and low-hPSU.

[5] Even for the identical specimen with a given thickness, the width of the Kiessig fringe as observed by XR is smaller than that by NR by about 10% at small q. This is partially due to the contribution of the depressed SLD in NR near silicon wafer but primarily to the difference in the critical edge q_c for NR and XR. The latter factor in turns arises from the difference in the SLD for NR and XR. The difference in the fringe width, however, decreases with inceasing q, indicating importance of the latter factor.

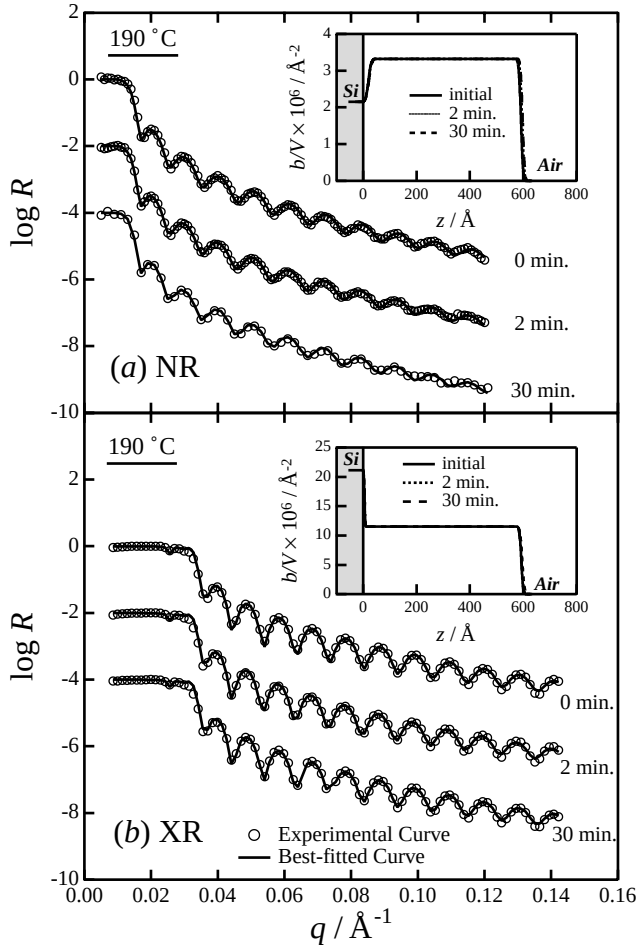

Fig. 2. NR (a) and XR profiles (b) (open circles) and the corresponding best-fit curves (solid lines) for the Si//dPSU-R/low-hPSU//Air system at different annealing times at 190°C. The (b/V) profiles, which correspond to the best-fit curves, are also shown as insets in the respective figures.

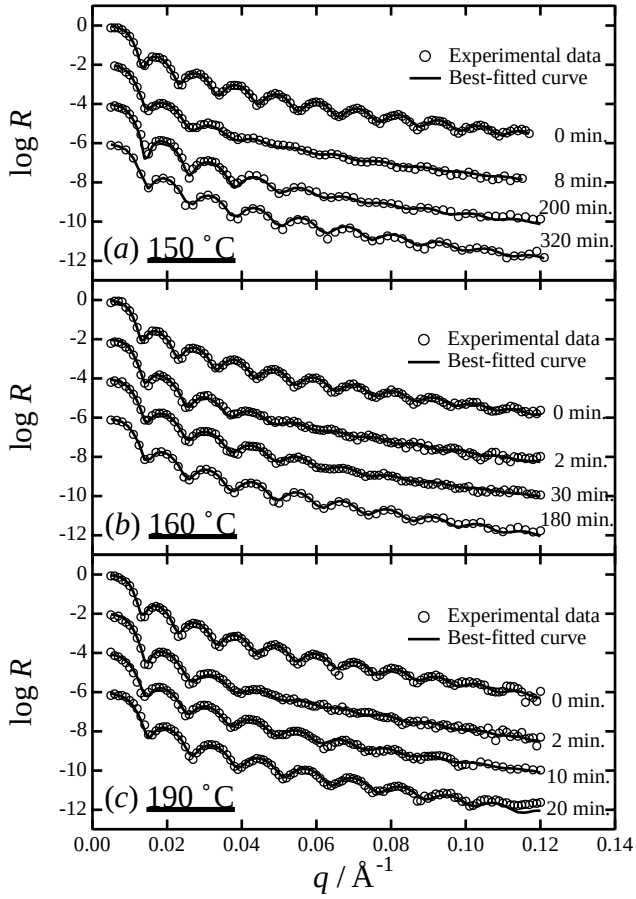

Fig. 3. NR profiles (open circles) and the corresponding best-fit curves (solid lines) for the Si//dPSU-R/low-hPSU//PA//Air system at various annealing times: (a) 150°C, (b) 160°C, and (c) 190°C, respectively.

3.3. NR characterization of bilayer specimens and the reactive blending process

Fig. 3 shows the time-dependent change of the NR profiles (open circles) during annealing at three different temperatures: (a) 150°C, (b) 160°C, and (c) 190°C, and the corresponding best-fit curves (solid lines) for the bilayer system of Si//dPSU-R/low-hPSU (30 wt%/70 wt%)//PA//Air. For all the annealing temperatures, a disappearance of most of the fringes at early annealing times is clearly observed. However, the disappeared fringes are recovered after longer annealing times (320 min in Fig. 2(a), 90 min in (b) and 20 min in (c)). These anomalous features observed in the bilayer film (Si//dPSU-R/low-hPSU//PA//Air) were not observed in the single layer films (Si//dPSU-R/low-hPSU//Air and Si//dPSU//low-hPSU//Air) as elucidated in Section 3.2. The rate of the recovery process increases with increasing temperatures. Another important feature is a greater fringe spacing than the initial state.

The SLD profiles obtained by fitting the NR data for different annealing times at the respective temperatures are shown in Fig. 4, where each curve corresponds to each best-fit curve in Fig. 3 (solid lines). In comparison with Figs. 3 and 4, two specific features, which are independent of annealing temperature, can be ascertained. First, when the fringes in the NR profile disappear in the course of initial annealing for several minutes, the interface between the PSU and PA layers becomes broader and also the SLD near the Si interface (at z around 50 Å) increases, physical origin of which will be discussed later in Section 4. Second, when the fringes in the NR profile return, the interface between the PSU and PA layer becomes sharp again and the PSU layer shrank. The shrinkage of the PSU layer is consistent with the increased fringe spacing as the fringes are little more than the Kiessig fringes for the dPSU-R layer. In addition to the shrinkage, the SLD of the PSU phase recovers the initial value, which will be also discussed in Section 4.

In order to check whether or not these features were unique to the reactive system, experiments were done with a non-reactive system as well. Fig. 5 shows the NR data for the Si//dPSU/low-hPSU//PA//Air (open circles) and the corresponding best-fit curves (solid lines) at various annealing times for the temperatures (a) 160°C and

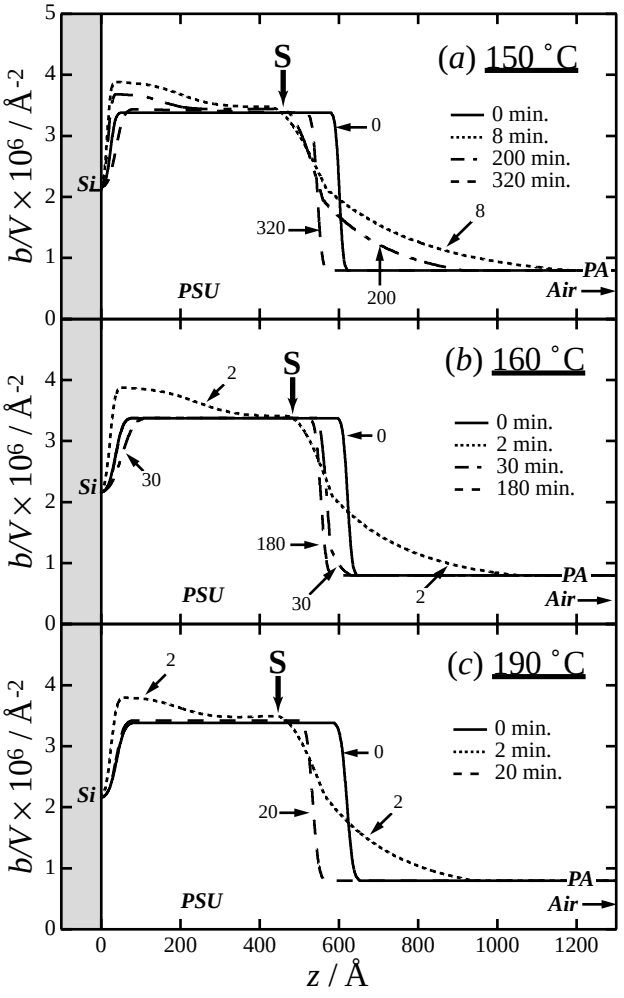

Fig. 4. SLD profiles corresponding to the best-fit curves for the NR data in Fig. 3 for the Si//dPSU-R/low-hPSU//PA//Air system.

(b) 190°C. The corresponding SLD profiles are shown in Fig. 6.

Looking at Figs. 5(a) and 6(a), the features are almost identical to the reactive system at 160°C. On the other hand, the NR data in Fig. 5b and the SLD profiles in Fig. 6b for the non-reactive system at 190°C exhibit behavior which is slightly different from the reactive analog at intermediate annealing times. Looking at Fig. 5b, the degree to which the fringes disappear and return is considerably less than in Fig. 3c. As seen in Fig. 6b, this corresponds to a substantially sharper interface. For both the reactive and non-reactive systems, the PSU layer shrinks. This means that transient broadening of the interface probably occurred in the non-reactive system, but the time scale over which it occurred is considerably shorter than 2 min at 190°C: for the reactive system, the time scale over which the interface instability occured is longer than 2 min at the same temperature. Hence, the formation of diblock in the reactive system may play a pivotal role on the kinetics of transient interfacial instability which will be discussed again in Section 4.

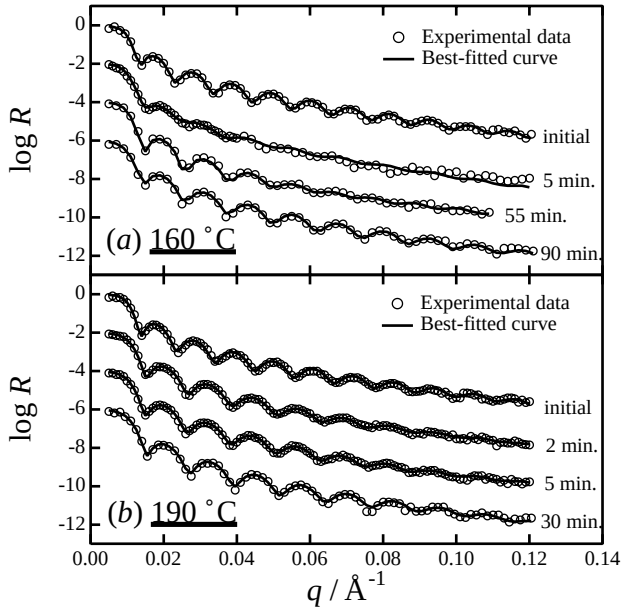

Fig. 5. NR profiles (open circles) and the corresponding best-fit curves (solid lines) for the Si//dPSU/low-hPSU//PA//Air system at the various annealing times at (a) 160°C and (b) 190°C, respectively.

4. Discussion

Putting dPSU-R/low-hPSU or dPSU/low-hPSU mixtures in contact with PA to form a bilayer PSU//PA specimen leads to transient interfacial instabilities upon annealing. During the instability, models for the NR data where low-hPSU diffuses into the PA layer and enriched near the interface while dPSU-R and dPSU consequently enrich near Si, giving rise to a higher value of SLD near Si, are consistent with the disappearance of the Kiessig fringes arising from the well-defined dPSU-rich layer in the unannealed sample. Upon relaxation of the instability, dPSU-R and dPSU enriched near Si subsequently interdiffuse in the PSU layer, and as a consequence the SLD of the PSU layer attains a uniform distribution with z with its value being slightly increased.[6] In addition to these changes, thickness of the PSU layer has decreased, indicating hydrogenous low-hPSU has been selectively extracted by PA. Here, it should be noted that the PA layer is thick enough to take up all miscible low-hPSU. Finally, reactive blending at elevated temperatures seems to decrease the lifetime of the instability. In the remainder of this section, three issues will be addressed: the origin of the interfacial instability (see Sections 4.1–4.3), comparisons between the reactive and non-reactive systems (see Section 4.4), and a comparison to previous work on similar systems (see Section 4.5).

[6] The values (b/V) attained after the recovery of the instability at 150 and 160°C were observed to be same as those in the initial state, though we estimate an increase of the value by about 5–6%, if dPSU-R does not diffuse out from the PSU layer into the PA layer, as will be discussed later in this section.

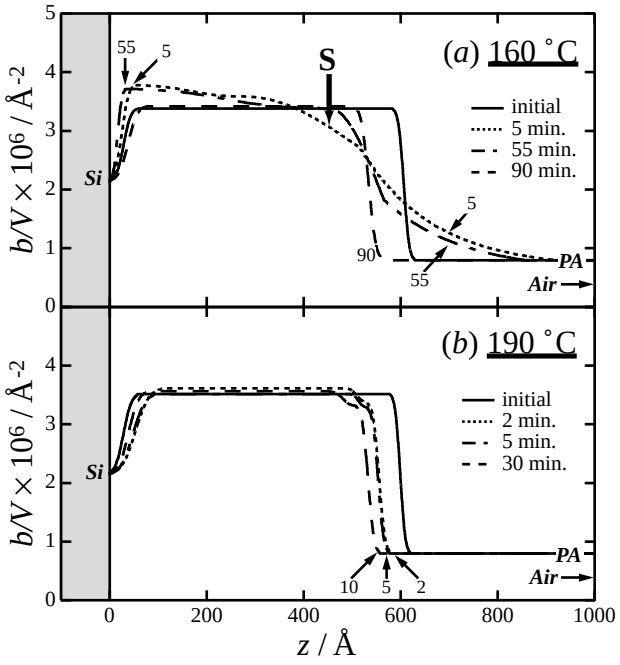

Fig. 6. SLD profiles corresponding to the best-fit curves for the NR data in Fig. 5 for the Si//dPSU/low-hPSU//PA//Air system.

4.1. Origin of the transient interfacial instability

The intriguing anomaly observed in the NR profiles was only present in the systems of Si//dPSU-R/low-hPSU//PA//Air and Si//dPSU/low-hPSU//PA//Air. Neither NR nor XR profiles revealed the anomaly for the single layer films of Si//dPSU-R/low-hPSU//Air. Additionally, a previous study for Si//dPSU-R/hPSU//PA//Air, which was essentially free of low-hPSU, and the system Si//dPSU-R//PA//Air only showed weak signatures of the transient instability [9]. Thus, the striking anomaly observed is definitely related to low-hPSU present in the PSU layer of the bilayer film. Here, let us discuss below what the anomaly implies in terms of the interface between the PSU layer and the PA layer.

If the lowest molecular weight fraction of low-hPSU is small enough, it can be miscible in PA, even though PSU and PA have a large repulsive segmental interaction parameter. Under this scenario, transient mass transport of the low molecular weight fraction of low-hPSU from the PSU layer to the PA layer would transiently change the interface between the bilayers, which in turn broaden the SLD profile across the interface. The SLDs for low-hPSU (hPSU), dPSU-R, and PA are 1.89×10^{-6}, 5.61×10^{-6}, and 7.96×10^{-7} Å^{-2}, respectively. Thus, the interdiffusion of low-hPSU can account for the transient change in the SLD profile. There are two possible models for the transient change in the interface, both of which can account for the change in number of Kiessig fringes and in the SLD profile: (i) uniform broadening of interface (the segmental density profiles across the interface being broadened uniformly everywhere along the interface) and (ii) undulation or corrugation of the interface. Both processes are followed by a recovery of a sharp and flat interface after completion of the mass transport or extraction of the low molecular weight fraction of the low-hPSU into the PA layer. According to this scenario, the transient interface instability occurs during the time period in which the low molecular weight fraction of the low-hPSU diffuses into the PA layer. The residual PSU remaining in the PSU layer posseses a higher molecular weight after extraction, which promotes a sharp interface between the strongly immiscible PSU and PA. Unfortunately, these above two possibilities (i) and (ii) cannot be distinguished from specular reflectivity measurements alone.

4.2. Analogous or relevant experiments concerning origin of the instability

Normally, NR experiments for semi-infinite systems (finite layer next to silicon, very thick 'infinite' layer on top) of miscible polymer bilayers leads to a rapid loss of number of Kiessig fringes [20] (corresponding to the thickness of the deuterium-rich layer) analogous to what is seen in the early stages of Figs. 3 and 5 [20]. This is due to the fact that the film once completely mixed is too thick to resolve the individual Kiessig fringes one would obtain from the total film thickness because of limitations on the q-resolution in NR experiments. What is surprising in the present study is that the Kiessig fringes return with a greater spacing.

This is analogous to, but different from, interdiffusion experiments with finite thickness samples. An example of this can be found in Fig. 7, where the system Air//hPS ($M_w = 39\times10^3$)//dPS ($M_w = 40\times10^3$)//Si is considered. As seen in the figure, the initial profile has strong NR Kiessig fringes (bumps) where the spacing is predominately determined by the thickness of the dPS layer. After just 5 min of annealing at 120°C, the fringes have more or less disappeared corresponding to a broad interface as seen in the corresponding SLD profile. Just as in Figs. 3 and 5, the fringes return; however, they are more closely spaced corresponding to a thicker uniform film with slight dPS adsorption at the Si and air interfaces. By analogy, the NR profiles seen in Figs. 3 and 5 for long annealing times must correspond to a SLD profile with a thinner homogeneous high SLD layer (dPSU or dPSU-R rich) as modeled.

The displacement of the interface is similar to Kirkendall effect experiments [21–23] in metals and marker displacement studies in polymeric systems [24–30]. In these experiments, the mismatch in the self-diffusivity is responsible for the displacement of the interface. In a more rigorous sense, our system may not directly correspond to either Kirkendall or marker experiments, as the bulk of the low-hPSU phase is immiscible with the PA. Although only a fraction of the low-hPSU is miscible with PA instead, the miscible fraction of low-hPSU has vastly different self-diffusivity against PA.

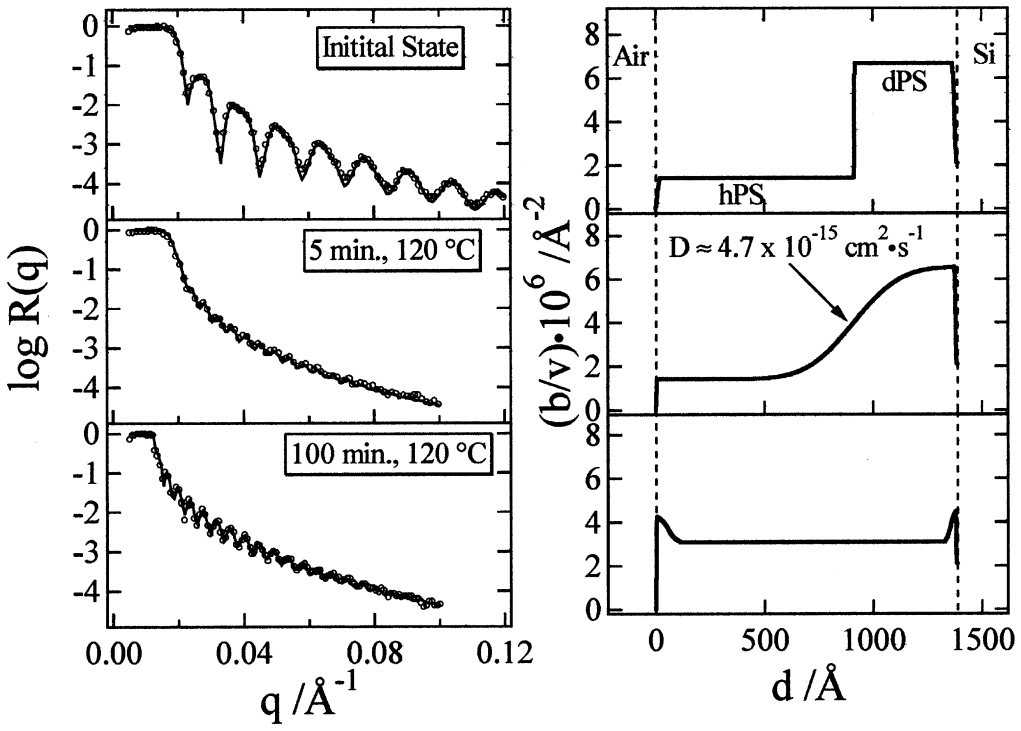

Fig. 7. Left hand graphs showing NR profiles (open symbols) and the corresponding best-fit curves (solid lines) for the Air//hPS ($M_w = 39 \times 10^3$)//dPS ($M_w = 40 \times 10^3$)//Si sytem at different annealing times. The graphs on the right hand side of the figure show the SLDs used to generate the best fit curves on the $R(q)$ vs. q plots.

In this sense, our system contains physical processes inherent to the Kirkendall or marker experiments and can be treated as a special case of the Kirkendal or marker experiments. Hence, the displacement is wholly ascribed to finite miscibility of a fraction of the low-hPSU with PA and to vastly different diffusivities between these two species.

To illustrate this, we consider an analogous sample comprised of Air//IPCC//dPS ($M_w = 1.55 \times 10^3$)/hPS ($M_w = 1.11 \times 10^6$)//Si. The logic here is that the dPS/hPS mixture will have low and finite miscibility with the rod-like IPCC matrix arising from unfavorable rod/coil mixing [31,32] and finite swelling of a cross-linked network [33,34]. Nonetheless, dPS having lower MW with a much faster diffusion coefficient should preferentially diffuse into and swell the IPCC-rich phase. Fig. 8 shows NR data and their corresponding SLD profiles for the Air//IPCC//dPS ($M_w = 1.55 \times 10^3$)/hPS ($M_w = 1.11 \times 10^6$)//Si system. One important difference in Figs. 3, 5 and 7 is that there is not a transient interfacial instability. For this system, the miscibility of dPS ($M_w = 1.55 \times 10^3$) and the finite cross-linked IPCC layer only leads to a slight damping of the NR fringes corresponding to a moderate broadening of the interface as seen in the SLD profiles. Nonetheless, time dependent displacement of the interfacial position is consistent with low molecular mass dPS swelling the membrane preferentially over the much larger hPS sample. This necessarily requires that the SLD of the IPCC layer increases and the SLD of the mixed PS layer decrease as is seen in Fig. 7. This experiment is completely consistent with the explanation that the PA layer extracts a miscible fraction of low-hPSU.

The similarity (the extraction of the miscible fraction of the low molecular weight species by the PA layer or the cross-linked IPCC layer) and the dissimilarity (with respect to the existence and non-existence of transient instability) in the behavior of the two systems may further infer the following interesting possibility. In the Air//IPC//dPS ($M_w = 1.55 \times 10^3$)/hPS ($M_w = 1.11 \times 10^6$)//Si system, the diffusion of the dPS may not involve the undulation or corrugation of the interface, because it costs an excess free energy due to the elastic deformation of the cross-linked IPCC layer, resulting in lack of creation of the transient interfacial instability during the diffusion process. Thus, the diffusion of the dPS is likely to occur only via the broadening of the interface that occurs uniformly along the interface. Thus, the transient interface instability, which is accompanied by the transient disappearance and recovery of the Kiessig fringes, observed in the PSU//PA bilayer might be due to the interface undulation rather than the uniform broadening of the interface. Again, this implication should be checked in future by other experimental methods. The dynamic asymmetry between the low molecular weight fraction of low-PSU and others (dPSU-R, dPSU or PA) may cause the stress-diffusion coupling and viscoelastic effect [35,36] during the diffusion process of the low molecular weight fraction of low-PSU in the PSU layer and the PA layer, which may promote the transient interface undulation. It is also conceivable that the transient drop of the local

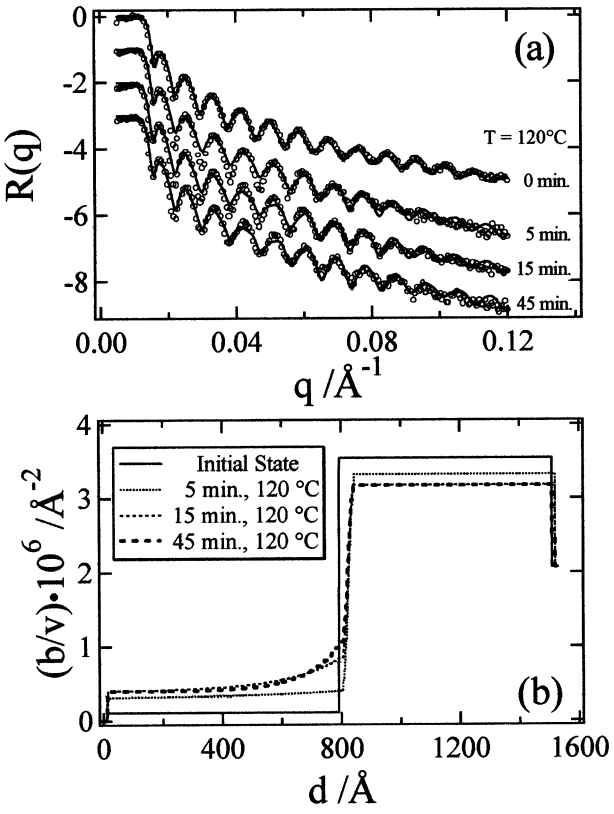

Fig. 8. (a) NR profiles (open symbols) and the corresponding best-fit curves (solid lines) for the Air//IPCC//dPS ($M_w = 1.55 \times 10^3$)/hPS ($M_w = 1.11 \times 10^6$)//Si system at different annealing times. (b) The SLD profiles used to generate the best-fit curves shown in (a).

interfacial tension due to the transient diffusion of the low molecular weight fraction of low-PSU may cause the transient undulation of the interface.

4.3. Fraction and molecular weight of low-hPSU that diffuses into the PA layer

The volume fraction of the low-hPSU that diffuses into the PA layer can be estimated from the change in the SLD profiles between the initial state and after long annealing times. In this estimation, it is assumed that only the low molecular weight fraction of the PSU diffuses into PA and both high molecular weight PSU and PA remain within their respective layers. This assumption was previously found to be qualitatively reasonable [10]. As shown in Fig. 9, the

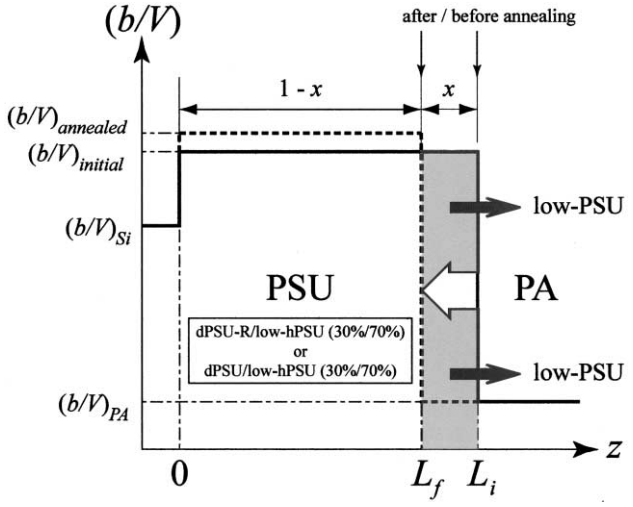

Fig. 9. Schematic illustration for a change in the SLD profile with annealing: before annealing (solid line) and after annealing and completion of the transient interface instability (dashed line).

thickness of the PSU layer before and after annealing, defined as L_i and L_f can be used to calculate the volume fraction, x, of the PSU which is miscible with PA ($x = (L_i - L_f)/L_i$). Based on this, x was estimated to be $x = 0.13$–0.14 for the reactive and $x = 0.11$–0.12 for the non-reactive system. These values are summarized in Table 4 for both systems at different temperatures. The fraction of the diffusing species within low-hPSU, defined as y, is estimated by $y = x/0.7 = (L_i - L_f)/(0.7L_i)$. This leads to values of $y = 0.18$–0.20 for the reactive system and $y = 0.16$–0.18 for the non-reactive system, where the y values at individual temperatures are also summarized in Table 4. Furthermore, the change in the SLD for the PSU layer accompanied by the diffusion can be estimated as follows: The SLD prior to annealing is given as $(b/V)_{initial} = 0.3(b/V)_{dPSU} + 0.7(b/V)_{low\text{-}hPSU}$ and the SLD after annealing is described by $(b/V)_{annealed} = [0.3/(1-x)](b/V)_{dPSU} + [1 - 0.3/(1-x)](b/V)_{low\text{-}hPSU}$ where $(b/V)_{dPSU}$ could equally well apply to dPSU-R. In the calculation of $(b/V)_{annealed}$, only low-hPSU was assumed to have a fraction which was miscible enough with PA to undergo complete diffusion, thereby providing a maximum estimate of the low molecular weight fraction in low-hPSU. Using the values for $(b/V)_{dPSU} = 5.61 \times 10^{-6}$ Å^{-2} (also applies to dPSU-R), $(b/V)_{low\text{-}hPSU} = 1.89 \times 10^{-6}$ Å^{-2}, and the x values given in Table 4, values of $(b/V)_{initial} = 3.00 \times 10^{-6}$ Å^{-2} for both the

Table 4
Fraction of low-hPSU which diffused into the PA layer after the complete relaxation of the instability ($x \equiv (L_i - L_f)/L_i$) and fraction of the diffused PSU in low-hPSU ($y \equiv x/0.7$)

Temperature (°C)	Reactive system Si//dPSU-R/low-hPSU//PA//Air					Non-reactive system Si//dPSU/low-hPSU//PA//Air				
	L_i (Å)	L_f (Å)	x	y	$(b/V)_{annealed} \times 10^6$ (Å^{-2})	L_i (Å)	L_f (Å)	x	y	$(b/V)_{annealed} \times 10^6$ (Å^{-2})
150	581	504	0.13	0.19	3.17	–	–	–	–	–
160	574	500	0.13	0.18	3.17	578	515	0.11	0.16	3.14
190	578	497	0.14	0.20	3.19	570	500	0.12	0.18	3.16

reactive and non-reactive systems, and $(b/V)_{\text{annealed}} = [3.18 \pm 0.01]$ and $[3.15 \pm 0.01] \times 10^{-6}$ Å^{-2} for the reactive and non-reactive systems were calculated, respectively. Hence, the SLDs are expected to increase only slightly after the diffusion (5–6%), which is within the experimental resolution of the NR technique in this work: after a precise anlaysis of the SLD profiles, we found that the SLD values thus estimated from Figs. 3 and 5 are subjected to errors of at least 5%. The variation of the SLD by 5% is negligibly small in the plots of Figs. 4 and 6. The experimental SLD values after annealing are nearly similar to or slightly greater than those prior to annealing, which is consistent with the picture described above.

Ideally, the molecular weight of the low molecular weight fractions of low-hPSU which are miscible with and diffuse into the PA phase could be analyzed by comparing GPC data for the PA layer before and after the complete relaxation of the interfacial instability upon annealing. The difference in the GPC data would highlight the molecular weights of the low-hPSU species, which actually diffused from the polysulfone phase into the PA phase. Although this experiment was not practically done, it is still possible to estimate the amount of low molecular weight impurities in low-hPSU from GPC data for the pure compound. GPC data show that low-hPSU contains a mass fraction of dimer equal to ca. 20%, the amount of which approximately corresponds to the fraction of the low-hPSU which diffused into the PA layer (see the quantity y in Table 4). Thus, the diffusing species of low-hPSU is expected to be dimers of PSU. This amount is almost independent of the annealing temperature T_a within experimental accuracy for both reactive and non-reactive systems, suggesting that the low-hPSU having a molecular weight greater than trimers is hardly miscible with PA at these temperatures.

According to this scenario, the transient interface instability occurs during the time period in which the low molecular weight fraction of the low-hPSU diffuses into the PA layer. The residual PSU remaining in the PSU layer posseses a higher molecular weight after extraction which promotes a sharp interface between the strongly immiscible PSU and PA.

4.4. Comparison between reactive and non-reactive systems

As a starting point, the general trend regarding the time dependent evolution of the interface while the interfacial instability occurs is considered. In order to compare the results obtained for the reactive and non-reactive systems, it is important to note that the reactive system definitely creates the block copolymer dPSU-*b*-PA as clarified elsewhere [9] and as will be discussed in Section 4.5. This can be seen in the time dependent evolution of the SLD shown in Figs. 4 and 6. Needless to say, the possibility that other SLD profiles can fit the NR data equally well, especially for the complicated profiles as shown in these figures [37–39], cannot be excluded. Furthermore, the SLDs shown in these figures represent apparent SLDs in the sense that the SLDs may reflect undulations of the interface and/or the broadening of the intrinsic interfacial thickness caused by mixing unlike species across the interface.

In both reactive and non-reactive systems, two stages for the transient instability can be seen: (1) an initiation and growth process, and (2) a relaxation process. In the initiation and growth process, the interface becomes broader with time, while it sharpens during the relaxation process. Differences between the two systems can be seen in the transient SLD profiles, especially in the profiles near the interface such as in the portion marked S in Figs. 4 and 6. The 'shoulder' marked by the arrow (S) is much clearer in the reactive system than in the non-reactive system. This difference may be due to localization of the block copolymers formed near the interface for the reactive system. It is also seen during the interface instability that the largest attainable SLD tail of PSU into the PA layer in the reactive system extends over a much larger distance than that in the non-reactive system. This tendency may be reasonable, at least qualitatively, from the viewpoint that the block copolymer formed in the reactive system tends to decrease the interfacial tension of the system and hence enhance the instability. This difference might favor the undulation model rather than the interfacial broadening model.

4.5. Comparison of the present results with previous results on Si//dPSU-R/hPSU//PA//Si

For the sake of comparison, Fig. 10 shows SLD profiles [9] measured by NR for the Si//dPSU-R/hPSU//PA//Air system at 210°C, which differs from the present study in terms of the PSU used as a diluent (hPSU vs low-hPSU) for the reactive component of dPSU-R. Here, only two profiles are shown, before and after annealing where thermal equilibrium is attained. Note that hPSU has a substantially higher molecular weight than low-hPSU

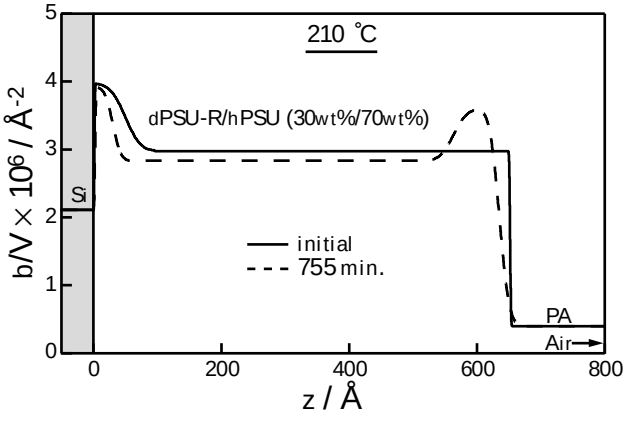

Fig. 10. Change in the SLD profiles with annealing time for the reactive system (Si//dPSU-R/hPSU(30 wt%/70 wt%)//PA//Air) at the annealing temperature of 210°C for a comparison with that shown in Figs. 4 and 6. Note that hPSU has much higher average molecular weights than low-hPSU in Figs. 4 and 6.

(Table 1). The detailed description and discussion of the result for hPSU in Fig. 10 is given elsewhere [9]. Fig. 10 is provided again for the sake of facilitating a comparison with the profiles in Figs. 4 and 6 in the long time limit after the relaxation of the instability.

Before comparing the two systems, the following points need to be made clear regarding the system with hPSU: (1) A mass fraction of a 2.5% of low molecular weight fractions in hPSU diffuse into the PA layer at 210°C, which is smaller than the system with low-hPSU (≈20%). (2) The transient interfacial instability was not observed after 10 min at annealing temperature $T_a = 210$°C in the matrix of hPSU/dPSU-R with $T_g \cong 184$°C or hPSU/dPSU with $T_g \cong 186$°C. For the latter point, this does not necessarily mean that the instability did not occur as it may have already completely relaxed. As it is not possible to compare the NR profiles at intermediate annealing times accompanying the instability, the comparison will focus on late annealing times.

Fig. 10 clearly reveals an enrichment of deuterium containing species in the SLD profile at the interface between the PSU and PA layers after annealing at 210°C due to the block copolymer formed at the interface via reactive blending as fully discussed elsewhere [9]. This is also expected to be the case for the reactive system with low-hPSU as a diluent at the T_as studied, as discussed in Section 4.4. However, in the system with low-hPSU, the block copolymers, dPSU-*b*-PA formed at the interface did not show up the enrichment of deuterium containing species in the SLD profile at the interface. How can we interpret this difference? Since molecular weight of hPSU is almost equal to that of dPSU-R, the block dPSU in the dPSU-*b*-PA formed at the interface behaves closely to the dry brushes against the hPSU [40]. On the other hand, molecular weight of low-hPSU is much smaller than that of the block dPSU in the dPSU-*b*-PA, the block dPSU definitely behaves as wet brushes against the low-hPSU [40]. Thus, it is well expected that the dPSU blocks having the high SLD are much more swollen by the low-hPSU than by the hPSU. Hence, the local concentration of dPSU and the enrichment of the SLD near the interface is expected to be much less in the low-hPSU than in the hPSU, which may account for the observed difference in the long time limit SLD profiles of the two systems near the interface with the PA layer.

We can estimate the excess local volume concentration of dPSU, $\Delta(z)$, attained in the system with hPSU as a diluent after the long annealing time at 210°C (for 755 min) from its initial concentration, $\bar{\phi}_{dPSU}$, on the basis of its local SLD profile $(b/V)_z$,

$$(b/V)_z = (b/V)_{dPSU}[\bar{\phi}_{dPSU} + \Delta(z)] + (b/V)_{hPSU}\{1 - [\bar{\phi}_{dPSU} + \Delta(z)]\} \quad (3)$$

where $\bar{\phi}_{dPSU} = 0.293$ can be estimated from the initial composition of dPSU of 30 wt%. We obtained $\Delta(z \cong 600\ \text{Å}) \equiv \Delta_1 = 0.184 \pm 0.025$ and $\Delta(100 \leq z \leq 500\ \text{Å}) \equiv \Delta_2 = -0.0255 \pm 0.017$, by taking fitting errors into account. Thus, we expect that the Δ value near the PA interface in the system of Si//low-hPSU/dPSU-R//PA//Air should be less than 0.018 (about 10% of Δ_1), judging from our experimental evidence of the non-enrichment of the SLD at the interface.

5. Conclusion

The NR studies of the bilayer films of Si//dPSU-R/low-hPSU//PA//Air during a reactive blending process revealed that fraction (~20 wt%) of small molecular weight low-hPSU (primarily composed of dimers) which are miscible with PA diffuse into the PA phase. This diffusion process is found to cause a shift of the average position of the interface toward the Si surface, resulting in a Kirkendall-like effect. We observed for the first time that this Kerkendall-like effect observe here is accompanied by a transient interfacial instability such that the number of NR fringes initially decreases with time and then return at later annealing times. The period over which the instability occurs essentially corresponds to the time scale for diffusion of dimers present in low-hPSU into the PA layer.

It is crucial to elucidate whether this transient interfacial instability occurs via transient capillary wave instabilities (undulations) of the interface, a transient increase in the interfacial width, or a combination of the two mechanisms. Unfortunately, it is not possible to distinguish between these two possibilities by specular NR studies alone. The clarification of this problem is crucial to unveiling of actual diffusion mechanisms of molecules across the interface of bilayer systems and confirming whether or not a conventional mean-field picture of the diffusion process occurs in experiments, especially for the systems with the dynamical asymmetry [35] in the component polymers, i.e. the low molecular weight fraction of the low-hPSU and others (dPSU-R and PA). The scenario of the undulation may be more favorable than the scenario of the uniform interfacial broadening from the discussion in Section 4.2 in conjunction with the results in Figs. 3, 5 and 8.

It should also be noted that specular NR studies alone cannot confirm or exclude whether the instability produces micelles of the dPSU-*b*-PA block copolymers, which are initially formed at the interface via end-group reactions, in the PSU or PA phases. Namely, the block copolymers formed at the interface may partially remain there solely as a monolayer or may partially aggregate into the micelles and diffuse into the PSU and/or PA phase during the course of the transient interfacial instability.

Acknowledgements

T.H. and M.W. gratefully acknowledge a partial financial

support by the German Ministry for Science (BMBF project 03N30283). One of us, H.G., would like to thank the Alexander von Humboldt Foundation for financial support.

References

[1] Lin EK, Wu W, Satija SK. Macromolecules 1997;30:7224.
[2] Feng Y, Weiss RA, Karim A, Han CC, Keiser H, Peiffer G. Macromolecules 1996;29:3918.
[3] Jiao J, Kramer E, Vos SD, Möller M, Koning C. Macromolecules 1999;32:6261.
[4] Koriyama H, Oyama HT, Ougizawa T, Inoue T, Weber M, Koch E. Polymer 1999;40:6381.
[5] Triacca VJ, Ziaee S, Barlow JW, Keskkula H, Paul DR. Polymer 1991;32:1401.
[6] Scott C, Macosko C. J Polym Sci, Part B — Polym Phys 1994;32:205.
[7] Lyu SP, Cernohous JJ, Bates FS, Macosko CW. Macromolecules 1999;32:106.
[8] Jiao JB, Kramer EJ, de Vos S, Moller M, Koning C. Polymer 1999;40:3585.
[9] Hayashi M, Grüll H, Esker AR, Weber M, Sung L, Satija SK, Han CC, Hashimoto T. Macromolecules 2000;33:6485.
[10] Hayashi M, Hashimoto T, Hasegawa H, Takenaka M, Grüll H, Esker AR, Weber M, Satija SK, Han CC, Nagao M. Macromolecules 2000;33:8375.
[11] Takeno H, Hashimoto T, Weber M, Schuch H, Koizumi S. Polymer 2000;41:1309.
[12] Weber M, Heckmann W. Polym Bull 1998;40:227.
[13] Joly R, Bucourt R, Mathieu J. Rec Trav Chim 1959;78:527.
[14] Rueggeberg WHC, Sauls TW, Norwood SL. J Org Chem 1955;20:445.
[15] Esker AR, Mengel C, Wegner G. Science 1998;280:892.
[16] Hasegawa H, Sakurai S, Takenaka M, Hashimoto T, Han CC. Macromolecules 1991;24:1813.
[17] de Gennes PG. Scaling concepts in polymer physics. Ithaca, NY: Cornell University Press, 1979.
[18] Flory PJ. Principles of polymer chemistry. Ithaca, NY: Cornell University Press, 1971.
[19] Co C, Welp KA, Wool RP. J Neutr Res 1999;8:37.
[20] Karim A, Felcher GP, Russell TP. Macromolecules 1994;27:6973.
[21] Smigelskas A, Kirkendall E. Trans Am Inst Min, Metall Pet Engng 1947;171:130.
[22] Lazarus D. In: Seitz F, Turnbull D, editors. Solid state physics, vol. 10. New York: Academic Press, 1960. p. 71.
[23] Tuijn C. Defect Diffus Forum 1997;141:1.
[24] Kramer EJ, Green PF, Palmstrøm CJ. Polymer 1984;25:473.
[25] Green PF, Palmstrøm CJ, Mayer JW, Kramer EJ. Macromolecules 1985;18:501.
[26] Koizumi S, Hasegawa H, Hashimoto T. Macromolecules 1990;23:2955.
[27] Reiter G, Huttenbach S, Foster M, Stamm M. Macromolecules 1991;24:1179.
[28] Liu Y, Reiter G, Kunz K, Stamm M. Macromolecules 1993;26:2134.
[29] Cole DH, Shull KR, Rehn LE, Baldo P. Phys Rev Lett 1997;26:5006.
[30] Cole DH, Shull KR, Baldo P, Rehn L. Macromolecules 1999;32:771.
[31] Flory PJ. Macromolecules 1978;11:1138.
[32] Ballauff MJ. Polym Sci Polym Phys Ed 1987;25:739.
[33] Flory PJ, Rehner J. J Chem Phys 1943;11:521.
[34] Flory PJ. J Chem Phys 1950;18:108.
[35] Doi H, Onuki A. J Phys II, Fr 1992;2:1631.
[36] Toyoda N, Takenaka M, Saito S, Hashimoto T. Polymer 2001;42:9193.
[37] Berk NF, Majkrzak CF. Phys Rev B — Condens Matter 1995;51:11296.
[38] Majkrzak CF, Berk NF, Dura JA, Satija SK, Karim A, Pedulla J, Deslattes RD. Physica B 1998;248:338.
[39] Majkrzak CF, Berk NF, Dura J, Satija SK, Karim A, Pedulla J, Deslattes RD. Physica B 1997;241:1101.
[40] Leibler L. Macromol Chem Macromol Symp 1988;16:1.